B-9-03 Extended Abstracts of the 2020 International Conference on Solid State Devices and Materials, VIRTUAL conference, 2020, pp99-100

Demonstration of Reservoir Computing Using a Ferroelectric Capacitor

Eishin Nako[1], Kasidit Toprasertpong[1], Ryosho Nakane[1], Zeyu Wang[1], Mitsuru Takenaka[1] and Shinichi Takagi[1]
[1]Department of Electrical Engineering and Information Systems, The University of Tokyo
7-3-1, Hongo, Bunkyo-ku, Tokyo 113-8656, Japan
Phone: +81-3-5841-6733 E-mail: nako@mosfet.t.u-tokyo.ac.jp

Abstract

We propose reservoir computing utilizing the memory effect and nonlinearity of an MFM ferroelectric capacitor. We experimentally demonstrate this computing function on time-series data by taking virtual nodes from time responses of polarization currents after applying voltage input. The experiments show the high memory capacity and the calculation ability, indicating that ferroelectricity of MFM capacitors contributes to the performance of reservoir computing as well as FeFETs.

1. Introduction

Reservoir computing, which is one of the frameworks of recurrent neural networks, is regarded as promising for edge computing, because of the low power consumption and the expectation of real-time learning [1, 2]. We have proposed the reservoir computing using a ferroelectric-gate FET (FeFET) as a physical reservoir for further reduced power consumption and have experimentally revealed high performance reservoir computing using FeFET due to the dynamic ferroelectric responses [3]. This study has indicated a contribution of charging/discharging current in FeFETs to the performance, suggesting the possible application of MFM capacitors, which can also yield charging/discharging currents associated with polarization reversal, to the same system. Compared with FeFETs, MFM capacitors can provide advantages of easier integration into CMOS system due to implementation in a back end process and much less area penalty due to 3D integration, as seen in the FeRAM integration. In this study, thus, we propose reservoir computing using an MFM capacitor, shown in Fig. 1 and experimentally demonstrate the operation by using a $Hf_{0.5}Zr_{0.5}O_2$ (HZO) MFM capacitor.

2. Experimental Details

The structure and process flow of an MFM capacitor using ferroelectric HZO and an MIM capacitor using dielectric HfO_2 in this experiment are shown in Fig. 2. The capacitor size was 80×80 μm^2. The device shows ferroelectricity in *P*-*V* hysteresis loops under voltage swing over 1.5 V, as shown in Fig. 3. To examine the possibility of reservoir computing shown in Fig. 1, the triangular input voltage waveforms, whose high/low peaks correspond to 1/0 digital inputs, as shown in Fig. 4(a), are applied to one terminal of the MFM capacitor. Then, the polarization response can be readout as the charging/discharging current, whose waveform is shown in Fig. 4(b). This transient and non-linear response of ferroelectric polarization in correspond to the triangular voltage input is expected to carry the function of the reservoir computing system [3]. The polarization current sampled at a constant time step is defined as virtual nodes. The product-sum of the virtual nodes and the weights ***w*** is carried out to calculate the output of the MFM-capacitor reservoir system. Here, V_{sw} of the waveform was varied to examine the impacts on the reservoir computing task performance.

2. Experiments and Results

In this study, we performed the Short Term Memory (STM) task to examine the memory of the recent input data at T_{delay} time-step back and the Parity Check (PC) task to examine the non-linearity, which are defined [5] by

$$y_{\mathrm{STM}}(t,T_{\mathrm{delay}}) = S_{\mathrm{in}}(t - T_{\mathrm{delay}}) \quad (1)$$

and

$$y_{\mathrm{PC}}(t,T_{\mathrm{delay}}) = S_{\mathrm{in}}(t - T_{\mathrm{delay}}) + \cdots + S_{\mathrm{in}}(t) (\mathrm{mod} 2) \quad (2)$$

respectively. After training the reservoir system (optimizing weight ***w***) by ridge regression for each task, the performance was evaluated by the memory capacity (MC) summed over T_{delay}, defined by

$$MC = \sum_{T_{delay}} Cor(T_{\mathrm{delay}})^2 = \sum \frac{Cov[y_{\mathrm{train}}(t,T_{\mathrm{delay}}), y_{\mathrm{out}}(t)]^2}{\mathrm{Var}[y_{\mathrm{train}}(t,T_{\mathrm{delay}})] \cdot \mathrm{Var}[y_{\mathrm{out}}(t)]} \quad (3)$$

where Cor means the correlation between the expected and the actual outputs. Note that the squared correlation becomes 1 in case of error-free and 0 in case that the training is failed.

Fig. 5 shows the squared correlation as a function of T_{delay} for the MFM capacitor with V_{sw} of 3 V and the time period of the input voltage waveform of 200 μs, together with the results of the MIM capacitor and the FeFET [3]. Here, the virtual node number (*N*) was taken to be 1000. Also, the numbers of the training and test data were 2000 and 500, respectively. It is found that the MFM capacitor exhibits the performance up to T_{delay} of 2 for both STM and PC tasks, different from the MIM one, which has no performance for T_{delay} higher than 1. This fact indicates that the time response of ferroelectric polarization in MFM contributes to reservoir computing. It is also found that the reservoir system using the MFM capacitor shows the similar performance to the FeFET one, indicating the ferroelectric reservoir system can be implemented in both forms. Fig. 6 shows the dependency of the number of virtual nodes from N = 5 to N = 1000 with V_{sw} of 3 V. The MC of the STM task of FeFET is saturated at N = 100, while that of MFM continues increasing from N = 5 to N = 1000. The MC of the PC task of both devices continues increasing from N = 5 to N = 1000. Fig. 7 shows the difference of the output current waveforms with different input voltage swings. The polarization switching peaks appear when V_{sw} > 1.5 V, as expected from the P-V hysteresis loops in Fig. 3. Fig. 8 shows the dependency of V_{sw} in the MC. The MC of the STM task increases with V_{sw}. In particular, the MC of the PC task significantly increases from 1.5 V where ferroelectric polarization starts to be observed.

Here, one thing needed to be careful when we evaluate MC is a memory effect in the input source and measurement systems. The generated input waveform may have a distortion due to finite values of parasitic capacitance or something. This distortion can cause a non-negligible memory effect in the input voltage waveform. Fig. 8 also shows the MC of the tasks only using the real input waveform, which was only monitored. It is found that while the STM task is affected by the memory effect of the input waveform, the PC task is not sensitive to this input memory effect. We can claim from these results that the MC of the PC task using the output waveform truly reflects the nonlinearity of the MFM devices. These findings confirm us that the ferroelectric polarization response is the main contribution of the reservoir computing using an MFM capacitor.

3. Conclusions

We have proposed reservoir computing by using the polarization time response of an MFM capacitor and have experimentally demonstrated that the reservoir computing performance originates from the ferroelectricity in HZO.

References [1] H. Jaeger, GMD Report, vol.148, 2001.
[2] W. Maass *et al.*, Neural Comp., vol.14, pp.2531–2560, 2002.
[3] E. Nako *et al.*, 2020 Symposia on VLSI Technology and Circuits, no.TN1.6, Jun.2020.
[4] L.Appeltant *et al.*, Nat. Commun, vol.1, pp.466-468, 2011.
[5] N. Bertschinger, Neural Comp., vol.16, pp.1413–1436, 2004.

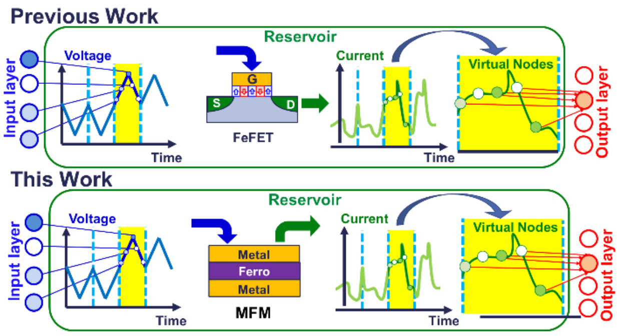

Fig.1 Proposed reservoir computing by using MFM

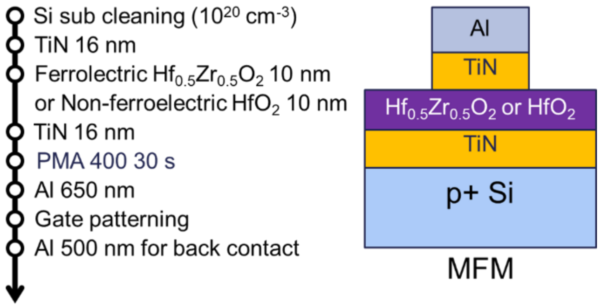

Fig. 2 Process flow and device structure of employed the MFM capacitor and the MIM capacitor.

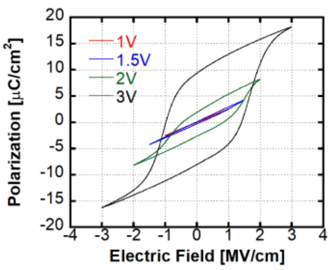

Fig. 3 *P-V* hysteresis loop of MFM capacitor.

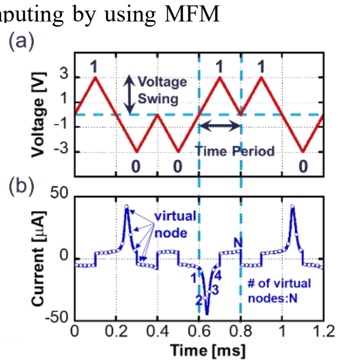

Fig. 4 (a) Voltage and (b) current waveforms of MFM capacitors for reservoir computing. Virtual nodes *N* are taken from current values.

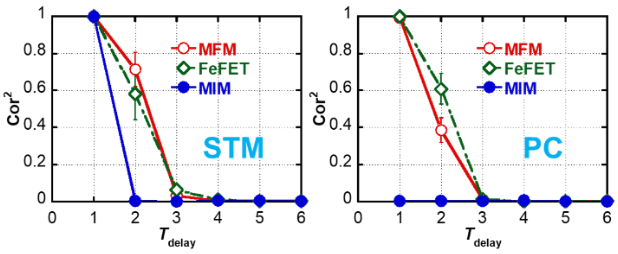

Fig. 5 Squared correlation (Cor^2) between the expected and actual outputs as a function of T_{delay} obtained from MFM and MIM capacitors, and FeFETs

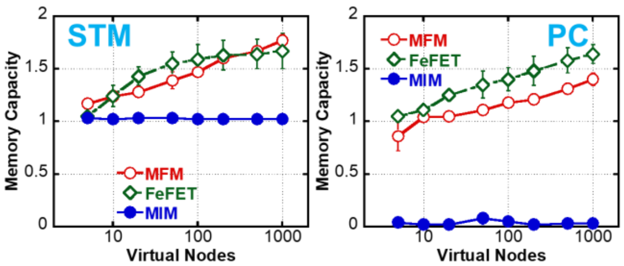

Fig. 6 Experimental MC of STM and PC as a function of virtual node number *N*

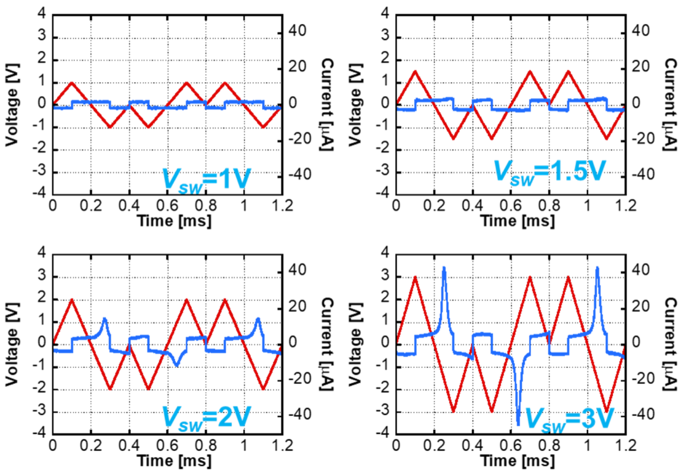

Fig. 7 Output current waveforms of MFM capacitors with input voltage swing V_{sw}

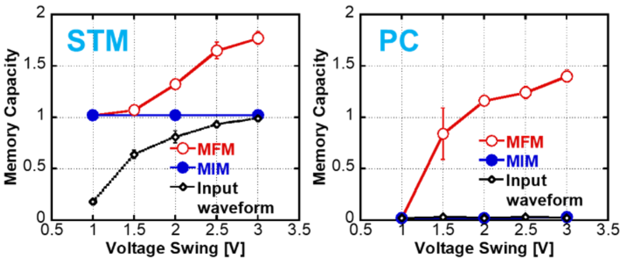

Fig. 8 Experimental MC of STM and PC as a function of V_{sw}